

# Preparation and properties of Nafion/SiO<sub>2</sub> composite membrane derived via *in situ* sol-gel reaction: size controlling and size effects of SiO<sub>2</sub> nano-particles

Chang-Chun Ke<sup>a,b</sup>, Xiao-Jin Li<sup>a\*</sup>, Shu-Guo Qu<sup>a,b</sup>, Zhi-Gang Shao<sup>a</sup> and Bao-Lian Yi<sup>a</sup>

A novel technique in controlling the size of SiO<sub>2</sub> nano-particles in the preparation of Nafion/SiO<sub>2</sub> composite membranes via *in situ* sol-gel method, as well as the effects of nano-particle size on membrane properties and cell performance, is reported in this paper. Nafion/SiO<sub>2</sub> composite membranes containing SiO<sub>2</sub> nano-particles with four different diameters ( $5 \pm 0.5$ ,  $7 \pm 0.5$ ,  $10 \pm 1$ , and  $15 \pm 2$  nm) are fabricated by altering the reactant concentrations during *in situ* sol-gel reaction. Sequentially, size effects of SiO<sub>2</sub> nano-particles on membrane properties and cell performance are investigated by SEM/EDAX, TEM, TGA, mechanical tensile, and single cell tests, etc. The results suggest that 10 nm is a critical diameter for SiO<sub>2</sub> incorporated into Nafion matrix, exhibiting desirable physico-chemical properties for operation at elevated temperature and low humidity. At 110°C and 59% RH, the output voltage of the cell equipped with Nafion/SiO<sub>2</sub> (10 nm) obtains an output voltage of 0.625 V at 600 mA/cm<sup>2</sup>, which is 50 mV higher than that of unmodified Nafion. Copyright © 2010 John Wiley & Sons, Ltd.

**Keywords:** proton exchange membrane fuel cell; *in situ* sol-gel; Nafion/SiO<sub>2</sub> composite membrane; SiO<sub>2</sub> nano-particle; size effect

## INTRODUCTION

Polymer electrolyte membrane fuel cell (PEMFC) is considered to be one of the most promising alternative energy conversion devices for motor vehicles and other stationary applications, due to its quick start, high energy efficiency, and environmentally friendly qualities.<sup>[1]</sup>

At present, most PEMFCs are operated at <80°C, due to the dependence of perfluorinated sulfonic acid membrane (such as Nafion<sup>®</sup> series) on water. Even so, operating PEMFC at a high temperature (>100°C) has many benefits.<sup>[2,3]</sup> Firstly, it avoids two-phase flow in the flow field, thus enhances the stability and reliability of PEMFCs system. Then, operating PEMFC at a high temperature reduces the power loss caused by the electro-chemical polarization of cathode. In addition, high temperature operation is also beneficial to make use of the exhaust heat of PEMFC system effectively and enhance the CO endurance of anode,<sup>[3]</sup> etc.

However, it is a pity that the most widely used commercial Nafion membrane is not competent for operating at high temperature due to dehydration. To solve this problem, many kinds of solutions have been proposed. One of the most widely investigated solutions is to incorporate hydrophilic or proton conductive inorganic nano-particles into the Nafion matrix to prepare so-called inorganic-organic composite membranes.<sup>[4–12]</sup> Many composite membranes of this type were reported in literatures, such as Nafion composite membranes with SiO<sub>2</sub>,<sup>[8,9,12–20]</sup> sulfonated-SiO<sub>2</sub>,<sup>[5]</sup> TiO<sub>2</sub>,<sup>[21,22]</sup> and ZrP,<sup>[23]</sup> etc.<sup>[24,25]</sup>

Among these composite membranes, Nafion/SiO<sub>2</sub> composite membrane was most extensively evaluated, and is promising. Several preparation methods have been reported, such as solution-recast route,<sup>[12]</sup> sol-gel method, self-assembling method,<sup>[15]</sup> *in situ* sol-gel method,<sup>[20,26]</sup> and so on. Among these methods, *in situ* sol-gel method is a promising route, because it can obtain composite membrane with smaller SiO<sub>2</sub> particles, and is easy to carry out. Mauritz *et al.*<sup>[13,27]</sup> first proposed this method, then Adjemian<sup>[26,28,29]</sup> and many other investigators<sup>[20,30]</sup> applied Nafion/SiO<sub>2</sub> composite membrane prepared by this or improved method to PEMFC and DMFC.

However, little work has been reported on how to control the diameter of SiO<sub>2</sub> nano-particles inside the Nafion/SiO<sub>2</sub> composite membrane, as well as size effects of nano-particles on the properties and PEMFC performance of composite membranes. Yuan *et al.*<sup>[16]</sup> investigated Nafion/HSS composite membranes containing hollow SiO<sub>2</sub> spheres with different

\* Correspondence to: X.-J. Li, Laboratory of Fuel Cell System and Engineering, Dalian Institute of Chemical Physics, Chinese Academy of Sciences, Dalian 116023, China.  
E-mail: xjli@dicp.ac.cn

a C.-C. Ke, X.-J. Li, S.-G. Qu, Z.-G. Shao, B.-L. Yi  
Laboratory of Fuel Cell System and Engineering, Dalian Institute of Chemical Physics, Chinese Academy of Sciences, Dalian 116023, China

b C.-C. Ke, S.-G. Qu  
Graduate School of Chinese Academy of Sciences, Beijing 100049, China

diameters in the range from 120 to 500 nm by re-casting method. Nevertheless, size controlling and the size effects of SiO<sub>2</sub> at a scale of ionic cluster of Nafion (about 5–10 nm under different states) are still in the dark.

In this paper, a novel technique in controlling the size of SiO<sub>2</sub> nano-particles in the preparation of Nafion/SiO<sub>2</sub> composite membranes via *in situ* sol–gel method was presented. Then these composite membranes were characterized by SEM/EDAX, TEM, TGA, mechanical analysis, single cell tests, and so on, to study the size effects of SiO<sub>2</sub> nano particles on the physico-chemical properties and PEMFC performance of Nafion/SiO<sub>2</sub> composite membrane.

## EXPERIMENTAL

### Composite membrane preparation

Nafion/SiO<sub>2</sub> composite membranes were prepared via an *in situ* sol–gel reaction of TEOS.<sup>[13]</sup> The detailed process is shown as follows. Firstly, the Nafion (NRE212 or 115) membrane (DuPont, USA) was dried in the vacuum drying oven at 80°C for 12 hr. Then, the membrane was dipped into the CH<sub>3</sub>OH/H<sub>2</sub>O solution (30°C) and kept for 1 hr. Afterwards, the sample was taken out and the remnant liquid on the surface of the membrane was rubbed out with filter paper. The sample was then immersed into CH<sub>3</sub>OH/TEOS solution (30°C) to carry out the *in situ* sol–gel reaction. The reaction time was 3 min for NRE212 and 5 min for Nafion 115. In this paper, four groups of reactant concentrations were adopted as shown in Table 1. After the reaction, the sample was kept in the vacuum drying oven at 80°C for 48 hr, and then Nafion/SiO<sub>2</sub> composite membrane was obtained.

Before the subsequent measurements, all the composite membranes were pretreated with the process as follows. Firstly, membranes were kept in H<sub>2</sub>O<sub>2</sub> (5 wt%, 80°C) for 1 hr, followed by rinsing them with de-ionized water (80°C) for two times. Then membranes were soaked in H<sub>2</sub>SO<sub>4</sub> (0.5 M, 80°C) for 1 hr. Finally, membranes were rinsed with de-ionized water (80°C) repeatedly until the PH of the washing water was around 7.

### SEM and EDAX analysis

A Philips XL-30TMP microscope was used to observe the cross-section morphology of the membranes, and an accessorial energy dispersive analysis of X-ray (EDAX) installation was used to analyze the Si elemental distribution across the composite membranes. The samples of membranes were cut with scalpel to expose their cross-sections.

### TEM

Transmission electron microscopy (TEM) was carried out to estimate the size of the *in situ* grown SiO<sub>2</sub> nano-particles.

**Table 1.** Conditions of reactant concentrations for preparing Nafion/SiO<sub>2</sub> composite membranes via *in situ* sol–gel reaction of TEOS

|                                      | I   | II  | III | IV  |
|--------------------------------------|-----|-----|-----|-----|
| CH <sub>3</sub> OH: H <sub>2</sub> O | 1:2 | 3:2 | 3:2 | 4:1 |
| CH <sub>3</sub> OH: TEOS             | 3:2 | 1:2 | 4:1 | 3:2 |

The Nafion/SiO<sub>2</sub> composite membranes were embedded into epoxy resin followed by ultra-microtomy with a diamond knife to obtain thin sections and placed on copper grids. The cross-section surface of the composite membrane was observed by a transmission electron microscope. TEM analysis was carried out using a JEM-2000EX (JEOL) microscope.

### Water-uptake measurements

For the water-uptake evaluation, to remove the residual water, the membrane was firstly dried in vacuum drying oven for 12 hr at 60°C. Then, the membrane was quickly taken out from the oven and weighed precisely. The weight of the dry membrane was signed as  $W_{dry}$ . After that, the membrane was soaked in de-ionized water at certain temperature (40, 60, or 80°C) for 24 hr. The weight of the wet membrane was signed as  $W_{wet}$ . The water-uptake (Wu) can be calculated by the following equation:

$$Wu = \frac{W_{wet} - W_{dry}}{W_{dry}} \times 100\% \quad (1)$$

### Swelling ratio measurements

The process of swelling ratio evaluation was similar to that of the water uptake evaluation. The dry length and wet length of the sample are signed as  $L_{wet}$  and  $L_{dry}$ , respectively. The swelling ratio (Sr) can be calculated by the following equation:  $(2) Sr = \frac{L_{wet} - L_{dry}}{L_{dry}} \times 100\%$

In this paper, the swelling ratios of Nafion and Nafion/SiO<sub>2</sub> membranes in de-ionized water at temperature of 40, 60, and 80°C were tested. In addition, swelling ratios of unmodified Nafion in CH<sub>3</sub>OH/H<sub>2</sub>O and CH<sub>3</sub>OH/TEOS solutions were also tested, at room temperature (298 K). For this purpose, CH<sub>3</sub>OH/H<sub>2</sub>O and CH<sub>3</sub>OH/TEOS solutions of certain concentration were used as swelling agents, respectively.

### Proton conductivity measurements

Electrochemical impedance spectroscopy (EIS) was carried out to measure the proton conductivity of the membranes using a PARSTAT<sup>®</sup> 2273 A (Princeton, USA) electrochemical system. The amplitude of the AC signal was 20 mV, and the frequency ranged from 100 Hz to 1 MHz. The sample was soaked in water at 55°C for 24 hr and then sealed between two stainless steel supported carbon paper electrodes with an area of 0.332 cm<sup>2</sup>. The conductivity can be calculated according to the following equation:  $(3) \sigma = \frac{L}{RA}$

where  $\sigma$  is the proton conductivity of the membrane,  $R$  is the resistance of the membrane, and the sign  $L$  and  $A$  are the thickness of the membrane and the area of the electrode, respectively. The impedance data were all corrected for the contribution of the empty cell and the interfacial resistance by intercept method.

### Mechanical tensile measurements

Mechanical tensile measurements were performed on a tensile tester WDW-01 (Kexin Instrument, Changchun) at room temperature in air. Tensile conditions were based on Chinese Standard QB-13022-91 and samples were tested at a programmed elongation rate of 50 mm min<sup>-1</sup>.

## Thermogravimetry analysis

The thermal stability of Nafion/SiO<sub>2</sub> composite membranes was analyzed by a STA 449F3 unit (NETZSCH, Germany), at a heating rate of 10 °C/min in air.

## MEA preparation and single cell test

All membrane electrode assemblies (MEAs) were prepared via a hot-pressing process. The gas diffused electrode (GDE) was prepared first by using carbon paper from Toray, 20 wt% Pt/C from E-TEK, PTFE suspension, and Nafion solution (DuPont, USA). The contents of Nafion and PTFE in the catalyst layer are both 23.6 wt%. The loadings of Pt/C catalyst on the anode and cathode were 0.4 mgPt/cm<sup>2</sup>. Then, two pieces of gas diffused electrode with effective area of 5 cm<sup>2</sup> were hot-pressed onto one piece of membrane to fabricate an MEA. The MEA was sandwiched into a single cell with stainless steel end plates and graphite groove flow fields as current collectors. The performance of the fuel cell was evaluated by polarization curve measurement at the temperatures of 60 and 110 °C, respectively. The H<sub>2</sub> and O<sub>2</sub> were fed into the fuel cell in co-flow mode. When the cell was operated at the temperature of 60 °C with fully humidified H<sub>2</sub>/O<sub>2</sub> gases, the flow rates of inlet gases were adjusted with current density to maintain the utilization of H<sub>2</sub> at 70% and O<sub>2</sub> at 40% for various current densities. When the cell was operated at the temperature of 110 °C with H<sub>2</sub>/O<sub>2</sub> gases and the relative humidity (RH) of 59%, the inlet gases were controlled at fixed flow rates of 35 and 100 ml/min respectively. All MEAs were evaluated under an absolute pressure of 0.3 MPa.

## RESULTS AND DISCUSSION

### Effects of reactant concentration on Nafion/SiO<sub>2</sub> preparation

*In situ* hydrolysis of TEOS during the Nafion/SiO<sub>2</sub> composite membrane preparation is a coupled diffusion-reaction process catalyzed by protons attached to sulfonic acid groups (–SO<sub>3</sub>H) of Nafion<sup>[27]</sup> as shown in Fig. 1. According to acknowledged “Cluster-Network” model of Nafion,<sup>[31]</sup> in Fig. 1, the sphere stands for the hydrophilic ionic cluster of swollen Nafion, which has been saturated with H<sub>2</sub>O and CH<sub>3</sub>OH in CH<sub>3</sub>OH/H<sub>2</sub>O solution. Once the swollen Nafion is immersed into CH<sub>3</sub>OH/TEOS solution, TEOS diffuses into the hydrophilic ionic cluster and reaches the sites of H<sup>+</sup>, which are also the collection location of water, and then the hydrolysis reaction occurs.

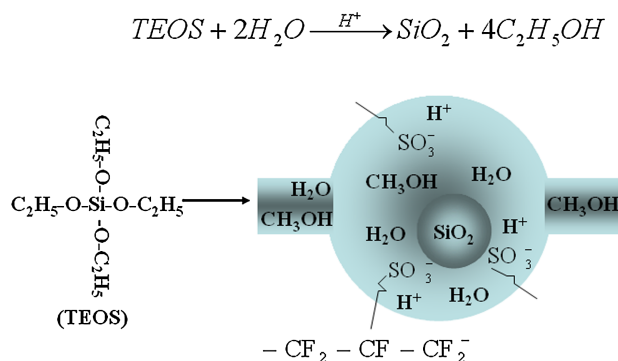


**Figure 1.** Schematic diagram of diffusion-reaction process of *in situ* hydrolysis of TEOS within the hydrophilic “ionic cluster” of Nafion. This figure is available in color online at [wileyonlinelibrary.com/journal/pat](http://wileyonlinelibrary.com/journal/pat)

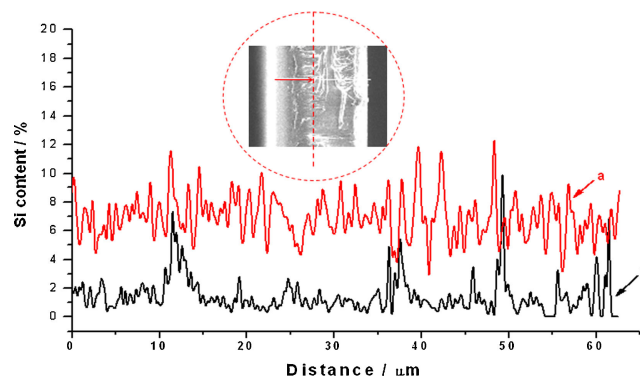
Figure 2 shows Si element distribution of Nafion115/SiO<sub>2</sub> composite membranes (across the membrane) prepared in our experiments, under different reactant concentrations: (a) TEOS: CH<sub>3</sub>OH = 3/2, CH<sub>3</sub>OH: H<sub>2</sub>O = 2/1; (b) TEOS: CH<sub>3</sub>OH = 2/3, CH<sub>3</sub>OH: H<sub>2</sub>O = 1/2. The reaction temperature was 30 °C, and the reaction time was 5 min. It can be seen from Fig. 2 that sample (a) has a higher content of SiO<sub>2</sub> than sample (b), and especially, Si element distribution across sample (b) is not as homogeneous as across sample (a), which could be concluded by comparison of the value of ΔSi%/Average (Si%), where ΔSi% means the gap between the highest and lowest Si% of the sample, and the Average(Si%) means the average value of Si% in the sample. For the sample (a), the value of ΔSi%/Average (Si%) is about 1.2, while for sample (b) the value of ΔSi%/Average (Si%) reaches 9.0. It reveals that the reactant concentrations indeed have a great effect on the distribution and micro-structure of SiO<sub>2</sub> nano-particles in the preparation of composite membrane.

It is generally believed that Nafion has a special structure with a hydrophilic ionic region scattering in hydrophobic domains, H<sub>2</sub>O and CH<sub>3</sub>OH diffuse principally via the hydrophilic passage.<sup>[32,33]</sup> During the Nafion/SiO<sub>2</sub> samples preparation, CH<sub>3</sub>OH percentage, either of CH<sub>3</sub>OH/H<sub>2</sub>O solution or of CH<sub>3</sub>OH/TEOS solution, has great effects in composite membrane preparation. On the one hand, it affects the rate of hydrolysis reaction. On the other hand, it affects the swelling degree of Nafion matrix, and thus the space and micro-structure of TEOS diffusion channel.

Figure 3 gives the swelling ratios of Nafion in CH<sub>3</sub>OH/H<sub>2</sub>O and CH<sub>3</sub>OH/TEOS solutions of different methanol concentrations, at room temperature (298K). Methanol is an excessive swelling agent, while water and TEOS are much moderate swelling agents for Nafion polymer. It can be seen from Fig. 3, in the considering region, the higher the CH<sub>3</sub>OH concentration, either of CH<sub>3</sub>OH/H<sub>2</sub>O or of CH<sub>3</sub>OH/TEOS, the higher the swelling ratio of Nafion. Higher swelling degree would make more wide channels for TEOS to diffuse into the PFSA matrix and more room for the growth of SiO<sub>2</sub> particles.

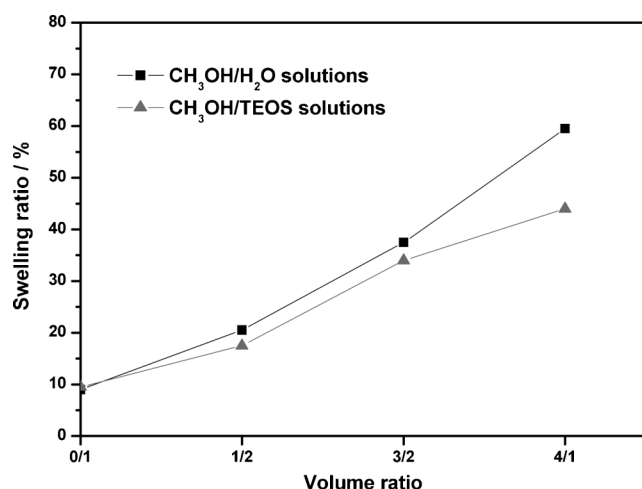
### TEM analysis and Diameter of SiO<sub>2</sub>

Figure 4 exhibits the TEM images of the four samples of composite membranes prepared at different reactant concentrations according to Table 1. The average diameter can be analyzed by *Image* software. During the four samples, Sample S(IV), possesses the maximal size of SiO<sub>2</sub> nano-particles, and has



**Figure 2.** Si element distribution (across the membrane) of Nafion115/SiO<sub>2</sub> composite membranes prepared via *in situ* sol-gel reaction under different reactant concentrations: (a) TEOS: CH<sub>3</sub>OH=3/2, CH<sub>3</sub>OH: H<sub>2</sub>O = 2/1 and (b) TEOS: CH<sub>3</sub>OH=2/3, CH<sub>3</sub>OH: H<sub>2</sub>O = 1/2. This figure is available in color online at [wileyonlinelibrary.com/journal/pat](http://wileyonlinelibrary.com/journal/pat)





**Figure 3.** Swelling ratios of Nafion in CH<sub>3</sub>OH/H<sub>2</sub>O and CH<sub>3</sub>OH/TEOS solutions of different volume ratios of V(CH<sub>3</sub>OH)/V(H<sub>2</sub>O) and V(CH<sub>3</sub>OH)/V(TEOS), respectively.

the average diameter of SiO<sub>2</sub> nano-particles of  $15 \pm 2$  nm. While, S(I), S(II), and S(III) have the average diameters of  $5 \pm 0.5$ ,  $7 \pm 0.5$ , and  $10 \pm 1$  nm, respectively. From the TEM analysis, it is proved that CH<sub>3</sub>OH/H<sub>2</sub>O and CH<sub>3</sub>OH/TEOS concentrations definitely

exert great influence on average diameter of SiO<sub>2</sub> nano-particles inside the Nafion/SiO<sub>2</sub> composite membrane. Table 2 shows the diameter of SiO<sub>2</sub> and the corresponding  $\Delta$ wt% (based on pure Nafion NRE212) in the four reaction conditions. It can be seen that the SiO<sub>2</sub> content incorporated into the composite membrane increases as the SiO<sub>2</sub> particle grows. It is necessary to note that, although  $\Delta$ wt% values of these four types of composite membrane are different from each other, the properties comparison (Water uptake, Swelling ratio, and Proton conductivity, etc.) among these composite membranes is feasible. Because, in the *in situ* sol-gel, the number of sulfonic acid groups is equal for the four different types of Nafion/SiO<sub>2</sub> composite membranes, so is the number of the SiO<sub>2</sub> nano-particles.

From the TEM analysis, it is seen that reactant concentrations have great impact in determining the diameter of SiO<sub>2</sub> nano-particles in preparation of Nafion/SiO<sub>2</sub> composite membrane via *in situ* sol-gel process. According to the mechanism of the effect of concentrations of reactants in determining the diameter of SiO<sub>2</sub> nano particles (discussed in section 3.1), it is easy to understand the size order of SiO<sub>2</sub> particles in samples as S(IV) > S(III) > S(II) > S(I). Comparison of those two CH<sub>3</sub>OH concentrations, the CH<sub>3</sub>OH concentration of CH<sub>3</sub>OH/H<sub>2</sub>O plays the leading role, because the time for samples kept in CH<sub>3</sub>OH/H<sub>2</sub>O (1 hr) is much longer than that of CH<sub>3</sub>OH/TEOS (3 min).

#### Water uptakes and swelling ratios of Nafion/SiO<sub>2</sub> composite membranes

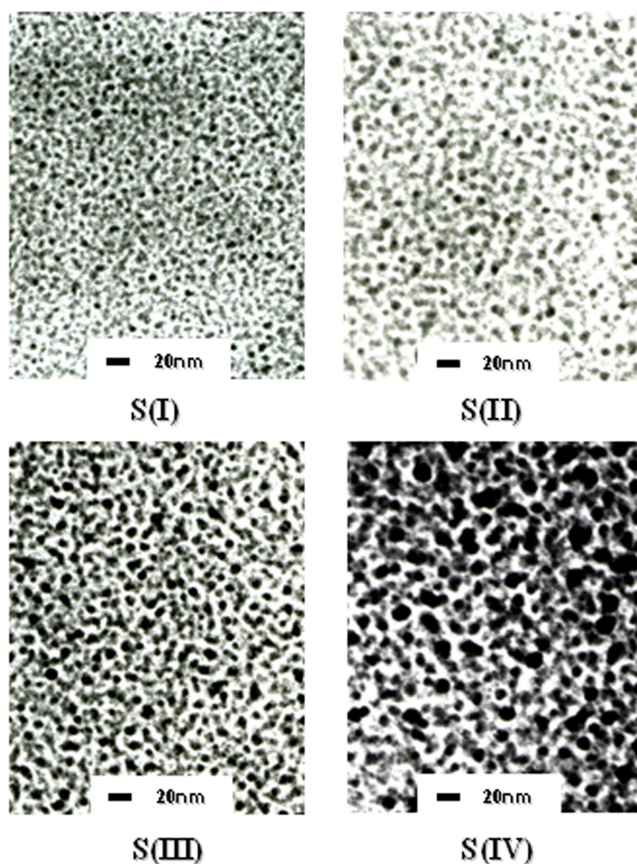
Figure 5(a) presents the water uptakes of Nafion/SiO<sub>2</sub> composite membranes in comparison to Nafion NRE212, at the temperatures of 40, 60, and 80 °C. It can be seen from Fig. 5(a) that all the Nafion/SiO<sub>2</sub> composite membranes show much higher water uptakes than the unmodified Nafion NRE212 at the appointed temperature region. It is due to the hydrophilic of SiO<sub>2</sub> nano-particles, possessing the capability of water maintenance.

Figure 5(b) exhibits swelling ratios of the Nafion/SiO<sub>2</sub> composite membranes in de-ionized water in comparison to Nafion NRE212. The swelling ratio of the unmodified Nafion NRE212 is 10%, and the swelling ratio of the membrane is raised after incorporation of SiO<sub>2</sub>. Especially, for Nafion/SiO<sub>2</sub>-15 nm, its swelling ratio is much higher than that of the unmodified Nafion membrane.

It is found that, as an increase in hydration, there is not an accompanying increase in the swelling ratio for the composite membranes. That should be caused by the different microstructure of the composite membranes, attributing to the different size of SiO<sub>2</sub> and thus interaction between nano fillers and polymer matrix.

#### Proton conductivities of Nafion/SiO<sub>2</sub> composite membranes

Figure 6 exhibits the proton conductivities of Nafion/SiO<sub>2</sub> composite membranes and Nafion NRE212 at fully hydrated states. It shows that proton conductivities of all the Nafion/SiO<sub>2</sub> composite membranes are lower than that of the unmodified Nafion NRE212. The conductivity loss of the composite membrane could be explained by the fact that SiO<sub>2</sub> is almost insulative for proton. From Fig. 6, it can also be seen, as the SiO<sub>2</sub> diameter increases from 5 nm to 10 nm, the proton conductivity of composite membranes grows. Nafion/SiO<sub>2</sub>-10 nm obtains the highest conductivity. But when the diameter increases further, the proton conductivity starts to decrease. It suggests that



**Figure 4.** TEM images of Nafion NRE212/SiO<sub>2</sub> composite membranes prepared under different reactant concentrations: S(I) CH<sub>3</sub>OH: H<sub>2</sub>O = 1/2, CH<sub>3</sub>OH: TEOS = 3/2; S(II) CH<sub>3</sub>OH: H<sub>2</sub>O = 3/2, CH<sub>3</sub>OH: TEOS = 1/2; S(III) CH<sub>3</sub>OH: H<sub>2</sub>O = 3/2, CH<sub>3</sub>OH: TEOS = 4/1; and S(IV) CH<sub>3</sub>OH: H<sub>2</sub>O = 4/1, CH<sub>3</sub>OH: TEOS = 3/2. This figure is available in color online at [wileyonlinelibrary.com/journal/pat](http://wileyonlinelibrary.com/journal/pat)

**Table 2.** Nafion/SiO<sub>2</sub> samples of various SiO<sub>2</sub> diameters prepared via *in situ* sol-gel process

|                         | Nafion/SiO <sub>2</sub> -5 nm | Nafion/SiO <sub>2</sub> -7 nm | Nafion/SiO <sub>2</sub> -10 nm | Nafion/SiO <sub>2</sub> -15 nm |
|-------------------------|-------------------------------|-------------------------------|--------------------------------|--------------------------------|
| A-Diameter <sup>a</sup> | 5 nm                          | 7 nm                          | 10 nm                          | 15 nm                          |
| ΔWt% <sup>b</sup>       | 6.5 ± 0.5%                    | 7 ± 0.5%                      | 8.5 ± 1%                       | 13.5 ± 1%                      |

<sup>a</sup> Average diameter of SiO<sub>2</sub> nano particles.  
<sup>b</sup> Weight percentage of SiO<sub>2</sub> incorporated into Nafion (based on pure Nafion).

~10 nm should be an appropriate diameter for SiO<sub>2</sub> incorporated into Nafion.

### Thermal stability and mechanical property analysis

The TGA curves of the Nafion/SiO<sub>2</sub> composite membranes and unmodified Nafion are shown in Fig. 7. For Nafion and Nafion/SiO<sub>2</sub> composite membranes, the weight loss before 298°C is due to residual water. Nafion started to decompose until 298°C, which is associated with the loosening of sulfonic acid groups. The difference of thermal stability caused by the incorporation of SiO<sub>2</sub> is negligible. That is because SiO<sub>2</sub> is well thermally stable as inorganic filler. In addition, from the results of TGA, the Nafion/SiO<sub>2</sub> composite membranes are stable enough for operation at elevated temperature (100–140°C) for HT-PEMFCs.

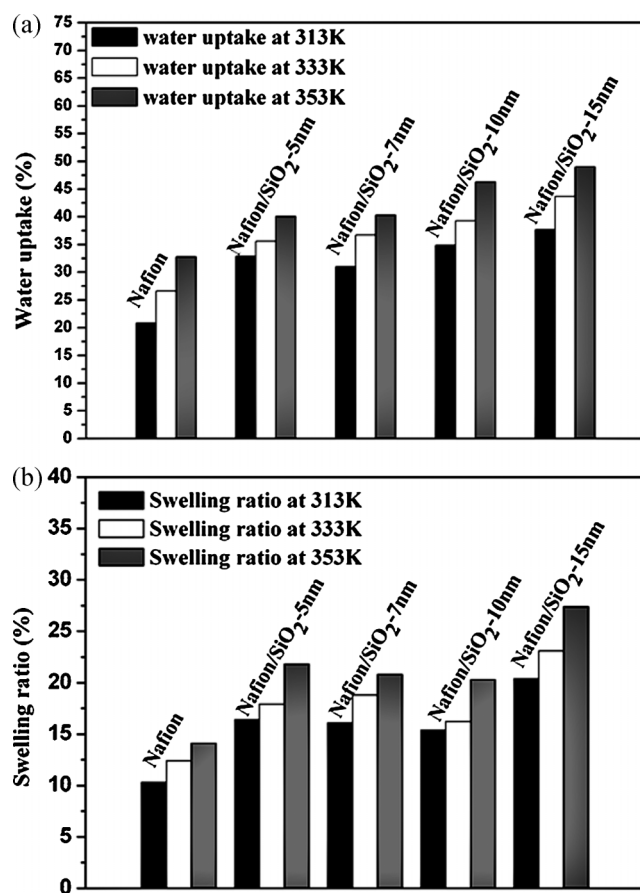


**Figure 5.** Water uptakes (a) and swelling ratios (b) of Nafion/SiO<sub>2</sub> composite membranes containing SiO<sub>2</sub> particles of a diameter of 5, 7, 10, and 15 nm, respectively.

Figure 8 exhibits the stress-strain curves of Nafion and Nafion/SiO<sub>2</sub> composite membranes. It shows that the incorporation of SiO<sub>2</sub> causes obvious tensile stress and elongation loss at break to Nafion. Especially, for Nafion/SiO<sub>2</sub>-15 nm, the tensile stress and elongation at break declines to 11.3 MPa and 55.3%, respectively. While, for Nafion, tensile stress and elongation at break is 25.2 MPa and 521.0%, respectively. The values are a little different from that provided by DuPont, maybe due to different testing conditions.

### Single cell performance

#### Low temperature and fully humidified performance

Figure 9(a) shows the polarization curves of the cells equipped with Nafion/SiO<sub>2</sub> composite membranes and unmodified Nafion NRE212 operated at 60°C, 100% RH. It shows that the composite membranes exhibit larger polarization loss than the unmodified Nafion NRE212 at this operating condition almost in the whole current density region. It should be caused by their lower proton conductivities in comparison to the unmodified Nafion membrane. As the SiO<sub>2</sub> diameter grows, the single cell performance of the composite membrane firstly ascends and then descends, showing almost the same trends of the proton conductivity as the SiO<sub>2</sub> diameter grows.

#### High temperature and low humidity performance

Figure 9(b) shows the polarization curves of the cells equipped with Nafion/SiO<sub>2</sub> composite membranes and unmodified Nafion NRE212 operated at 110°C, 59% RH. At this high temperature and low humidity, the water-retaining capability of the hydrophilic SiO<sub>2</sub> nano particles works. In the low current density region

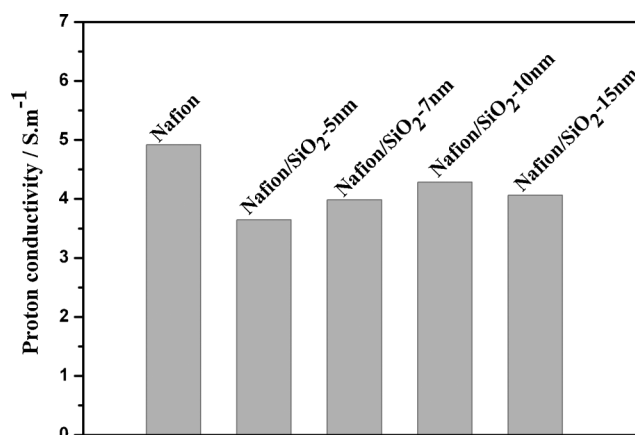


**Figure 6.** Proton conductivities of Nafion/SiO<sub>2</sub> composite membranes containing SiO<sub>2</sub> particles of a diameter of 5, 7, 10, and 15 nm, respectively.

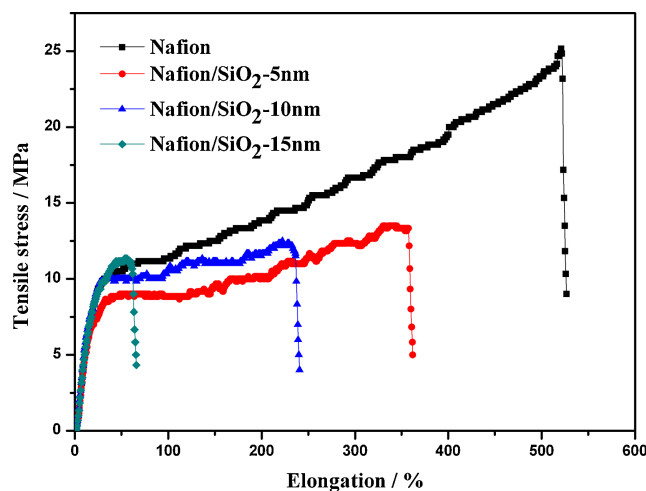


**Figure 7.** Stress–elongation curves of Nafion/SiO<sub>2</sub> composite membranes containing SiO<sub>2</sub> particles of a diameter of 5, 10, and 15 nm, respectively. This figure is available in color online at [wileyonlinelibrary.com/journal/pat](http://wileyonlinelibrary.com/journal/pat)

(<100 mA/cm<sup>2</sup>), the performance enhancement is not obvious. However, when it comes to medium and high current density region (>300 mA/cm<sup>2</sup>), the composite membranes exhibit obvious cell performance improvement compared to the unmodified Nafion NRE212. That should be due to the water-retain capability of SiO<sub>2</sub> nano particles. From Fig. 9(b), it can be seen that performance of Nafion/SiO<sub>2</sub>-15 nm is better than that of Nafion/SiO<sub>2</sub>-10 nm in the high current density region (>800 mA/cm<sup>2</sup>) at 110°C, 59% RH. However, when the current density is less than 800 mA/cm<sup>2</sup>, both performances are almost the same, and are higher than that of Nafion/SiO<sub>2</sub>-5 nm and Nafion/SiO<sub>2</sub>-7 nm. That is because the water-uptake capability grows gradually with the increase of SiO<sub>2</sub> diameter. Compared the cell performance of Nafion/SiO<sub>2</sub>-15 nm to Nafion/SiO<sub>2</sub>-10 nm, no further great improvement on cell performance was observed. This is because the conductivity loss of the composite membrane offsets the water-uptake improvement when the diameter of SiO<sub>2</sub> nano particles increases further. In addition, Nafion/SiO<sub>2</sub>-10 nm possesses lower swelling ratio and better mechanical properties

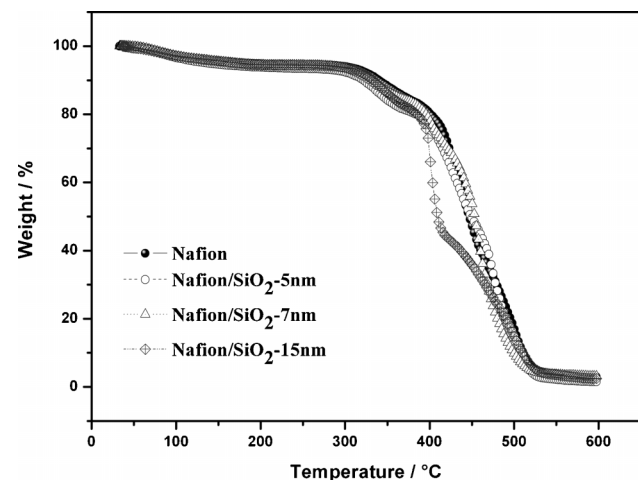


**Figure 8.** TGA curves of unmodified Nafion and Nafion/SiO<sub>2</sub> composite membranes with different diameter of SiO<sub>2</sub>. This figure is available in color online at [wileyonlinelibrary.com/journal/pat](http://wileyonlinelibrary.com/journal/pat)

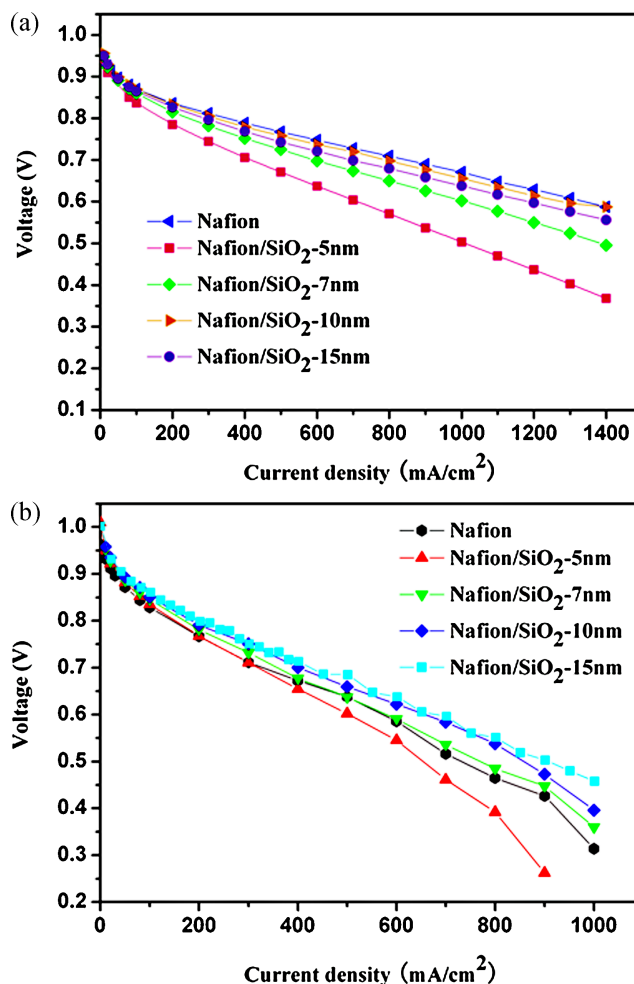


**Figure 9.** Polarization curves of single cells equipped with Nafion/SiO<sub>2</sub> composite membranes containing SiO<sub>2</sub> particles with diameters of 5, 7, 10, and 15 nm, respectively, at 60°C and 100% RH (a), and 110°C and 59% RH (b). This figure is available in color online at [wileyonlinelibrary.com/journal/pat](http://wileyonlinelibrary.com/journal/pat)

than Nafion/SiO<sub>2</sub>-15 nm. That is favorable for application in PEMFCs. Therefore, considering the water uptake, swelling ratio, proton conductivity, and cell performance of Nafion/SiO<sub>2</sub> composite membrane together, Nafion/SiO<sub>2</sub> composite membrane with SiO<sub>2</sub> nano-particles of an average diameter of 10 nm is a good choice for application in HT-PEMFCs.

## CONCLUSION

In this work, a technique in controlling diameter of SiO<sub>2</sub> nano-particles in preparation of Nafion/SiO<sub>2</sub> composite membranes was put forward. Nafion/SiO<sub>2</sub> composite membranes containing SiO<sub>2</sub> nano-particles with different diameters ( $5 \pm 0.5$ ,  $7 \pm 0.5$ ,  $10 \pm 1$ , and  $15 \pm 2$  nm) were prepared by controlling reactant concentrations of the *in situ* sol–gel reaction. Size effects of the SiO<sub>2</sub> nano-particles on physicochemical properties and cell performances of Nafion/SiO<sub>2</sub> composite membranes were analyzed by TEM, EIS, water uptake measurements, single cell tests, etc. The results show that composite membranes with SiO<sub>2</sub> nano-particles of 10 nm possess desirable properties and PEMFC performance at high temperature and low humidity, and reach an

output voltage of 0.625 V at 600 mA/cm<sup>2</sup>, at 110°C and 59% RH, which is 50 mV higher than that of the unmodified Nafion NRE212 membrane. This work studied the size effects of SiO<sub>2</sub> nano particles on the physicochemical properties of composite membrane, which is beneficial for understanding the preparation processes of Nafion/SiO<sub>2</sub> composite membrane via *in situ* sol gel reaction.

## Acknowledgements

This work was financially supported by the National High Technology Research and Development Program of China (863 Program No. 2007AA05Z131) and the National Natural Science Foundation of China (No. 20206030).

## REFERENCES

- [1] Marban, G. Vales-Solis, T. *Int. J. Hydrogen Energ.* **2007**, 32, 1625–1637.
- [2] Li, Q. F. He, R. H. Jensen, J. O. Bjerrum, N. J. *Chem. Mater.* **2003**, 15, 4896–4915.
- [3] Yang, C. Costamagna, P. Srinivasan, S. Benziger, J. Bocarsly, A. B. *J. Power Sources* **2001**, 103, 1–9.
- [4] Yan, X. M. Mei, P. Mi, Y. Z. Gao, L. Qin, S. X. *Electrochem. Commun.* **2009**, 11, 71–74.
- [5] Wang, L. Zhao, D. Zhang, H. M. Xing, D. M. Yi, B. L. *Electrochem. Solid-State Lett.* **2008**, 11, B201–B204.
- [6] Adjemian, K. T. Dominey, R. Krishnan, L. Ota, H. Majsztrik, P. Zhang, T. Mann, J. Kirby, B. Gatto, L. Velo-Simpson, M. *et al. Chem. Mater.* **2006**, 18, 2238–2248.
- [7] Mauritz, K. A. Mountz, D. A. Reuschle, D. A. Blackwell, R. I. *Electrochim. Acta* **2004**, 50, 565–569.
- [8] Wang, K. P. McDermid, S. Li, J. Kremliaikova, N. Kozak, P. Song, C. J. Tang, Y. H. Zhang, J. L. Zhang, J. J. *J. Power Sources* **2008**, 184, 99–103.
- [9] Jung, G. B. Weng, F. B. Su, A. Wang, J. S. Yu, T. L. Lin, H. L. Yang, T. F. Chan, S. H. *Int. J. Hydrogen Energ.* **2008**, 33, 2413–2417.
- [10] Costamagna, P. Yang, C. Bocarsly, A. B. Srinivasan, S. *Electrochim. Acta* **2002**, 47, 1023–1033.
- [11] Shao, Z. G. Xu, H. F. Li, M. Q. Hsing, I. M. *Solid State Ionics* **2006**, 177, 779–785.
- [12] Shao, Z. G. Joghee, P. Hsing, I. M. *J. Membrane Sci.* **2004**, 229, 43–51.
- [13] Mauritz, K. A. Warren, R. M. *Macromolecules* **1989**, 22, 1730–1734.
- [14] Yen, C. Y. Lee, C. H. Lin, Y. F. Lin, H. L. Hsiao, Y. H. Liao, S. H. Chuang, C. Y. Ma, C. C. M. *J. Power Sources* **2007**, 173, 36–44.
- [15] Tang, H. Wan, Z. Pan, M. Jiang, S. P. *Electrochem. Commun.* **2007**, 9, 2403–2408.
- [16] Yuan, J. J. Zhou, G. B. Pu, H. T. *J. Membrane Sci.* **2008**, 325, 742–748.
- [17] Jin, Y. G. Qiao, S. Z. Xu, Z. P. da Costa, J. C. D. Lu, G. Q. *J. Phys. Chem. C* **2009**, 113, 3157–3163.
- [18] Jin, Y. G. Qiao, S. Z. Zhang, L. Xu, Z. P. Smart, S. da Costa, J. C. D. Lu, G. Q. *J. Power Sources* **2008**, 185, 664–669.
- [19] Rodgers, M. P. Shi, Z. Q. Holdcroft, S. *J. Membrane Sci.* **2008**, 325, 346–356.
- [20] Liu, Y. H. Yi, B. L. Zhang, H. M. *Chin. J. Power Sources* **2005**, 29, 92–94, 112.
- [21] Tian, J. H. Gao, P. F. Zhang, Z. Y. Luo, W. H. Shan, Z. Q. *Int. J. Hydrogen Energ.* **2008**, 33, 5686–5690.
- [22] Santiago, E. J. Isidoro, R. A. Dresch, M. A. Matos, B. R. Linardi, M. Fonseca, F. C. *Electrochim. Acta* **2009**, 54, 4111–4117.
- [23] Alberti, G. Casciola, M. Capitani, D. Donnadio, A. Narducci, R. Pica, M. Sganappa, M. *Electrochim. Acta* **2007**, 52, 8125–8132.
- [24] Alberti, G. Casciola, M. *Annu. Rev. Mater. Res.* **2003**, 33, 129–154.
- [25] Jones, D. J. Rozière, J. *Handbook of Fuel Cells—Fundamental, Technology and Applications* (Eds: W. Vielstich, A. Lamm, H. A. Gasteiger), vol. 3 John Wiley & Sons, New York, **2003**, 447–455.
- [26] Adjemian, K. T. Lee, S. J. Srinivasan, S. Benziger, J. Bocarsly, A. B. *J. Electrochem. Soc.* **2002**, 149, A256–A261.
- [27] Mauritz, K. A. Stefanithis, I. D. Davis, S. V. Scheetz, R. W. Pope, R. K. Wilkes, G. L. Huang, H. H. *J. Appl. Polym. Sci.* **1995**, 55, 181–190.
- [28] Adjemian, K. T. Srinivasan, S. Benziger, J. Bocarsly, A. B. *J. Power Sources* **2002**, 109, 356–364.
- [29] Adjemian, K. T. Srinivasan, S. Bocarsly, A. B. *Abstr. Paper Am. Chem. Soc.* **2001**, 221, U382–U382.
- [30] Yu, J. Pan, M. Yuan, R. Z. *J. Wuhan Univ. Technol. Mater. Sci. Ed.* **2007**, 22, 478–481.
- [31] Gierke, T. D. Munn, G. E. Wilson, F. C. *J. Polym. Sci. Pol. Phys.* **1981**, 19, 1687–1704.
- [32] Verbrugge, M. W. *J. Electrochem. Soc.* **1989**, 136, 417–423.
- [33] Divisek, J. Eikerling, M. Mazin, V. Schmitz, H. Stimming, U. Volkovich, Y. M. *J. Electrochem. Soc.* **1998**, 145, 2677–2683.